RICHARD J. NUNGE
WILLIAM N. GILL

Mechanisms Affecting Dispersion and Miscible Displacement

Mechanisms influencing dispersion of solute material in another miscible phase in porous media consisting of several microstructure models

The nature of dispersion or miscible displacement in porous media may be examined from both an overall, or macroscopic, and a local, or microscopic, viewpoint. Because of the complexities of the structure of such media, there are difficulties associated with both approaches. Overall behavior, such as the average concentration distribution at the system outlet as a function of time, can be observed in sets of experiments, as is frequently done in practice, and the results can be correlated with the variables investigated on empirical or semiempirical bases. Such studies make up a large fraction of the existing work on miscible displacements in the literature. However, the generality of such results is questionable unless accompanied by a unifying theory.

To date, no theory which accounts for all the effects present in porous media has been established, and perhaps not even all the effects have been delineated. To construct macroscopically correct laws for describing miscible displacements, a knowledge of local behavior is required, since integral results which reflect overall behavior are obtained from integrating the differential equations which are assumed to describe local behavior. At this point in the development, it is assumed that the microscopic equations of change are accurate enough to describe phenomena as they occur in a porous medium. However, the application of these equations to porous media is difficult. Consider the flow boundaries in even the most orderly packed bed, and the geometric complexities are clear.

Perhaps the theory of transport in porous media will never reach a predictive level and will always remain closely linked with experiment for final parametric evaluation, just as the theory of turbulence relies heavily on experimental results. To improve the present situation, the need for more physically realistic models and more refined experimental evidence is clear.

This review describes the progress made in one attempt to examine the mechanisms influencing the dispersion of solute material in another miscible phase in porous media. The medium is considered to consist of a microstructure made up of the pores and void spaces in and between the solid materials. Because the geometry of the microstructure is generally too complex to be described by a single model, it is broken into several different types of models. This requires that the important mechanisms controlling the transport be identified through experiment so that realistic microstructure models may be developed.

Finally, the microscopic results need to be combined and averaged so that a comparison with macroscopic behavior can be attained. At this crucial point, the theory is intimately related to experiment since, like turbulence, it is necessary to combine experimental measurements with theoretical formulations to find the values of undetermined parameters. One of the main difficulties associated with this final step is that the physical structure of the media may contribute effects which are not easily included in the microscopic analysis and yet which contribute in a significant manner to the overall process. These include channeling and backmixing for example. Hence, most of the material discussed here relates to the microstructure models and cannot be applied to porous media without modification.

General Comments about Dispersion

When two miscible liquids are contacted and mixed as in a miscible displacement process, there can be no equilibrium except that of one phase uniformly distributed throughout the second. Hence, all of the phenomena of interest are transient. The process of distributing one phase in the second may be termed dispersion. In a forced flow, many modes of transfer

contribute to the overall process. These include longitudinal and transverse molecular diffusion and/or Knudsen diffusion, eddy diffusion if the flow is turbulent, free and forced convection, and surface tension–driven flows. In addition, the nature of the dispersion may be affected by the boundary conditions, flow pulsations, and, most significantly in a porous medium, geometrical configuration.

Here we shall be primarily concerned with the influence of these factors in simple configurations, but reference will be made to similar behavior in porous media, and some of the implications of the results for the simplified models toward studies in porous media will be pointed out. In all cases, the bounding material—*e.g.*, the solid phase making up the porous medium—is considered stationary and inert.

We shall restrict our discussion to binary systems that can be described by a continuum model and, in this case, the general partial differential equation which describes the dispersion process is

$$\frac{\partial C_A}{\partial t} + \nabla \cdot \bar{n}_A = r_A \tag{1}$$

If the flow is laminar this can be written as

$$\frac{\partial C_A}{\partial t} + (\nabla \cdot C_A \bar{v}) = \nabla \cdot \rho D \nabla \omega_A + r_A \tag{2}$$

where

C_A = mass concentration of component A
$\bar{v}$ = vector representing mass average velocity
ρ = density of the system
D = molecular diffusion coefficient
ω_A = mass fraction of A
r_A = reaction rate at which A is produced
$\bar{n}_A$ = vector representing mass flux of A
∇ = del operator

This equation applies to the local behavior of component A, and its solution provides one with a complete map of the mass concentration distribution of A throughout the system. However, even for dispersion in simple, well-defined systems, such as fully developed laminar flow in circular tubes, Equation 1 is difficult to solve analytically.

For systems of complex configuration such as porous media, Equation 1 is probably impossible to solve directly. Therefore, it is desirable to consider an alternate approach in which one settles for less information, which is also less exact, than that provided by a direct solution of Equation 1. Thus, appeal is made to the dispersion model which provides a good approximation to the cross-sectional area average of C, C_m, if the system is sufficiently long so that the residence time is large enough—*i.e.*, the dispersion model is asymptotic in time and applies only after sufficient time has passed since the process was started.

Complex geometrical configurations complicate the solution of Equation 1 in two important ways. First, it is difficult or perhaps impossible to determine the velocity field, $\bar{v}$, accurately. Second, boundary conditions become complex and difficult to deal with.

Much experimental work on miscible displacement in porous media has been interpreted and correlated on the basis of an equation identical in form to the one-dimensional unsteady-state diffusion equation:

$$\frac{\partial C_m}{\partial t} = E \frac{\partial^2 C_m}{\partial x_1^2} \tag{3}$$

with the molecular diffusion coefficient replaced by an effective longitudinal diffusion coefficient or dispersion coefficient E; x_1 is a space coordinate in the direction of main flow which moves with the mean interstitial velocity. The solution of Equation 3 with a step change in the inlet concentration, C_0, is well known to be

$$C_m/C_0 = 1/2\left[1 - \operatorname{erf}\left(\frac{x_1}{2\sqrt{Et}}\right) + \exp\left(\frac{u_m(x_1 + u_m t)}{E}\right)\left(1 - \operatorname{erf}\frac{x_1 + 2u_m t}{2\sqrt{Et}}\right)\right] \tag{4}$$

The exponential term in Equation 4 decays rapidly and hence, for sufficiently large times, Equation 4 plots as a straight line on arithmetic probability paper. Since E is usually an unknown, it is necessary to perform experimental measurements to determine its value. Available experimental evidence has been obtained mostly by measuring the effluent concentration as a function of time. This is then plotted as suggested by Equation 4 and the dispersion coefficient is determined from the following relationship (*67*).

$$E = \frac{1}{t}\left[\frac{L'}{3.625}\right]^2 \tag{5}$$

Here L' is the mixing length, or as defined by Taylor (*67*), the axial distance over which the average concentration of the displacing fluid changes from 10% to 90% of its inlet value. After E has been determined for several systems, it is assumed that this parameter is of value for extrapolation to similar situations.

One of the main deficiencies of this procedure is that experimental results have seldom followed the straight line on probability paper predicted by Equation 4, although this is generally ignored, perhaps because deviations may be ascribed to experimental error.

The lumped parameter model described above leaves much to be desired from a mechanistic point of view. The requirements to be imposed on a complex system before Equation 3 can be used with confidence have not been established on a firm theoretical basis. Much

---

AUTHORS *R. J. Nunge and W. N. Gill are members of the faculty of Clarkson College of Technology, Potsdam, N. Y. 13676, where Dr. Gill is Professor and Dr. Nunge is Associate Professor of Chemical Engineering.* *The work for this paper was supported by the Office of Saline Water.*

of the work reviewed here is addressed to this problem in simple geometries to establish such a basis under many conditions similar to those encountered in porous media.

Laminar Dispersion in Capillary Tubes

Perhaps the simplest model for the microstructure is the straight tube. Bundles of straight capillaries have long been used to model flow through porous media (*12*, *61*), and assemblages of randomly oriented straight pores or capillaries, where it is assumed that the path of a marked element consists of a sequence of statistically independent steps, direction and duration of which vary in a random manner, have been suggested by de Josselin de Jong (*22*), Saffman (*57–59*), and Scheidegger (*61*). Here the results of capillary dispersion are considered for the purpose of illustrating the interactions of some of the factors influencing miscible displacements in porous media. The straight tube provides a well-defined hydrodynamical system where the dispersion process is most easily described while still retaining many of the main features of the same process in porous media.

Consider first the dispersion of two fluids of the same constant physical properties in a straight capillary tube with steady fully developed laminar flow prevailing. An early experimental work which demonstrated the essence of the process without mathematical treatment was reported by Griffiths (*35*) in 1911, who observed that a tracer injected into a stream of water spreads out in a symmetrical manner about a plane in the cross section which moves with the mean speed of flow. As Taylor (*66*, *67*) pointed out, this is a rather startling result for two reasons. First, since the water near the center of the tube moves with twice the mean speed of flow and the tracer at the mean speed, the water near the center must approach the column of tracer, absorb the tracer as it passes through the column, and then reject the tracer as it leaves on the other side of the column. Second, although the velocity is unsymmetrical about the plane moving at the mean speed, the column of tracer spreads out symmetrically. The concentration of the tracer material is described by the two-dimensional unsteady convective diffusion equation, Equation 6.

$$\frac{\partial C}{\partial t} + u(r)\frac{\partial C}{\partial x} = D\left(\frac{\partial^2 C}{\partial x^2} + \frac{1}{r}\frac{\partial}{\partial r}\,r\,\frac{\partial C}{\partial r}\right) \tag{6}$$

Here C is the point concentration, u the parabolic laminar velocity profile, and x and r the axial and radial coordinates, respectively. Taylor showed that for a large enough number of times the process could be described by a one-dimensional dispersion model, as given in Equation 7.

$$\frac{\partial C_m}{\partial t} + u_m\frac{\partial C_m}{\partial x} = k\frac{\partial^2 C_m}{\partial x^2} \tag{7}$$

Upon defining a coordinate which moves with the mean speed of flow as

$$x_1 = x - u_m t \tag{8}$$

Equation 7 becomes

$$\frac{\partial C_m}{\partial t} = k\frac{\partial^2 C_m}{\partial x_1^2} \tag{9}$$

and therefore Equation 9 is simply the one-dimensional unsteady diffusion equation to which solutions are readily available under a variety of conditions. The molecular diffusion coefficient has been replaced by an effective axial diffusion coefficient or dispersion coefficient which, in the absence of axial molecular diffusion, Taylor showed to be

$$k = \frac{4a^2u_m^2}{192D} \tag{10}$$

where a is the tube radius. This simple equation provides a great deal of physical insight into the nature of the dispersion process if we interpret the numerator to be a measure of axial convection and the denominator to reflect the intensity of transverse mixing rather than just transverse molecular diffusion.

In this event, we see that the dispersion coefficient, which is a measure of the rate at which material will spread out axially in the system, is enhanced by having large differences in velocity exist across the flow and by taking place in equipment with large transverse dimensions. In contrast, any mechanism which increases transverse mixing, such as turbulence or transverse convection currents, reduces the dispersion coefficient. These arguments apply, in a qualitative way, to porous media as well as to simple configurations. That is, in porous media, dispersion is created by both the microscopic differences in velocity which exist in the interstices between particles and by large-scale or macroscopic effects such as channeling.

Aris (*4*) later extended the analysis to include axial molecular diffusion and demonstrated that the dispersion coefficient for this case contains Taylor's result with an additive term due to diffusion:

$$k = D + \frac{4a^2u_m^2}{192D} \tag{11}$$

This combined result will be referred to as the Taylor-Aris theory.

It is important to note the restriction placed on the Taylor-Aris theory with respect to time, since, unless this time is exceeded, the mean concentration distribution is not described by a dispersion model. For porous media, the dimension in the flow direction must be large enough to ensure sufficient residence time for a dispersion model to apply. Otherwise, measured dispersion coefficients, together with the solution to Equation 3, could not be used to predict the average concentration distribution.

Gill (*28*, *29*) has developed an analytical solution of the time-dependent convective diffusion equation which can be used to predict local concentrations at times large enough so that the dispersion model holds—*i.e.*, the solution is asymptotic in time in the same sense as the

Taylor-Aris theory. The basis for computing the local concentration is an expansion of the point concentration in a Taylor series about the mean concentration as given in Equation 12.

$$C_A = C_m + \sum_{n=1}^{\infty} f_n(\tau,y) \frac{\partial^n C_m}{\partial x_1{}^n} \qquad (12)$$

The dispersion model, Equation 9, and the nth derivative of Equation 9 with respect to x_1,

$$\frac{\partial^{n+1} C_m}{\partial x_1{}^n \partial t} = k \frac{\partial^{n+2} C_m}{\partial x_1{}^{n+2}} \qquad (13)$$

are used along with Equation 12 in the full convective diffusion equation, Equation 6 for example, to generate an infinite set of equations for the f_n functions. The dispersion coefficient is determined from the first-order function and appears in the problem as an eigenvalue. Note that Equation 13 assumes that k is not a function of axial distance. For dispersion in straight tubes, the dispersion coefficient obtained by this procedure agrees with the Taylor-Aris theory (Equation 11). The first three terms in Equation 12 are needed to give good agreement with the finite difference experiments (*1*) in the mixing zone $0.3 < x/(2u_m t) < 0.7$, while the higher order terms correct the local concentration in the extremes of the mixing zone. This procedure has also been generalized to include time-dependent velocity fields and has been employed in a variety of miscible displacement problems, as will be discussed later.

A complete description of the mechanisms controlling dispersion in a capillary tube as a function of dimensionless time and Peclet number is available from the finite difference solution of the full convective diffusion equation obtained by Ananthakrishnan *et al.* (*1*) for a step change in inlet concentration and by Gill and Ananthakrishnan (*31*) for the slug stimulus. Consider, for illustrative purposes, a slug of solvent A injected at time zero into a fully developed laminar flow of B. The initial configuration is shown in Figure 1*a*.

Different mechanisms dominate the transport process depending on the amount of time elapsed since it was initiated—*i.e.*, four-time regimes exist in which different mechanisms are most important. These are: (*a*) at very short times after injection, except at high flow rates, the dispersion of A into B takes place by pure axial molecular diffusion because of the high axial concentration gradients established. Thus, for a very short time, which is usually too brief to be of practical interest, the dispersion takes place as if the two phases were stagnant.

Since diffusive length is proportional to the square root of time and convective length to the first power, (*b*) at slightly higher times axial convection participates significantly in the dispersion. At high flow rates, axial convection is the controlling mechanism, and Figure 1*b* shows the distortion of the solvent slug into a parabolic shape when convection controls. From this it is clear that the action of axial convection is to establish large radial concentration gradients and hence (*c*) at slightly higher times, radial molecular diffusion contributes to the dispersion process. Note that A is now transported radially toward the wall at the front of the slug and toward the centerline at the rear of the slug, the result being a mixed zone of varying concentration as shown in Figure 1*c*.

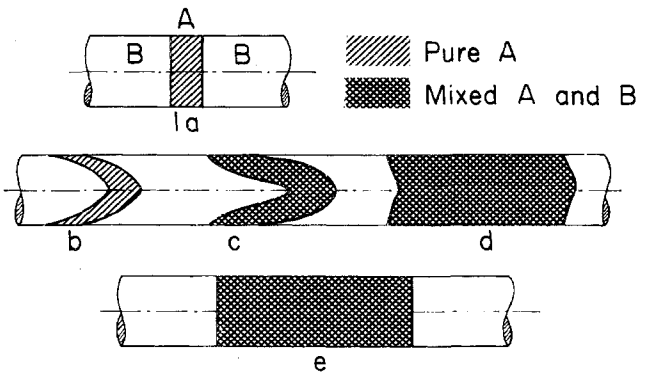

Figure 1. Schematic representation of the mixed zone for a slug of A dispersing in B as a function of time, A-B completely miscible

As time goes on, the action of radial diffusion convection continues to inhibit axial dispersion by diffusion and convection and makes the mixed zone more uniform as shown in Figure 1*d*. Finally, (*d*) at higher times, a pseudoequilibrium is established, Figure 1*e*, in which all three mechanisms contribute to the dispersion with the net effect appearing as if the fluid were in plug flow, whereas in fact the velocity is radially distributed. For this and higher times, the dispersion model results of the Taylor-Aris theory apply. As time increases further, the only effect is an increase in the length of the mixed zone.

The mechanisms are the same for the step change in inlet concentration (which occurs frequently in miscible displacements) as they are for a slug input; the mixed zones shown in Figure 1*c* through 1*e* then have concentrations varying between 1% and 99% A with all material to the left of the rear contour being pure A. Slight differences in the time required to reach the pseudoequilibrium region exist for the two types of experiments described above, as will be discussed later.

A graphical summary of the regions of applicability of various analytical solutions for dispersion for the step change in inlet concentration is given in Figure 2 with the dimensionless time and the Peclet number as parameters. Information on the intermediate range of parameters is provided (*1*). An important point relating to the dispersion model is that one finds that the dimensionless time $\tau = tD/a^2$ must be sufficiently large for it to apply—say 0.8 for fully developed laminar flow in tubes. Consequently the real time required is

$$t \approx \frac{0.8a^2}{D}$$

This simple formula provides us with a fairly general qualitative picture of when the dispersion model is

likely to apply if we interpret "a" as a typical transverse dimension of a system and D to be a measure of transverse mixing rates which may be caused by turbulence or convection in addition to molecular diffusion. In this event, we see that the real time required for the dispersion model to apply increases rapidly with an increase in the transverse dimension and is decreased by greater transverse mixing. Therefore, for example, we could expect the dispersion model to apply more generally to turbulent than to laminar systems.

The mixing length, L', the axial distance required for the average concentration of displacing fluid to change from 10% to 90% of its inlet value, is of critical importance in determining the usefulness of the displacement since, in general, it is desirable to keep the two phases as separate as possible (minimize axial dispersion). For large enough values of time, Taylor's analysis and the finite difference results of Ananthakrishnan *et al.* yield

$$L = \frac{DL'}{2a^2u_m} = 0.26\left(\frac{tD}{a^2}\right)^{1/2}, \quad \tau = \frac{tD}{a^2} > 0.8$$

Bailey and Gogarty (*7*, *8*) report a different exponent for the dimensionless time, but this evidently can be associated with inaccuracies in their numerical procedure (*1*). For small values of time, the mixing length results are correlated by

$$L = 0.8\,\tau, \quad \tau < 0.01$$

For small Peclet numbers the numerical results of reference 1 are correlated by

$$L = 2.5N_{Pe}^{-0.75}\,\tau^{0.55}, \quad \tau > 0.05 \qquad (14)$$

$$L = 2.5N_{Pe}^{-0.75}\,\tau^{0.60}, \quad \tau < 0.05 \qquad (15)$$

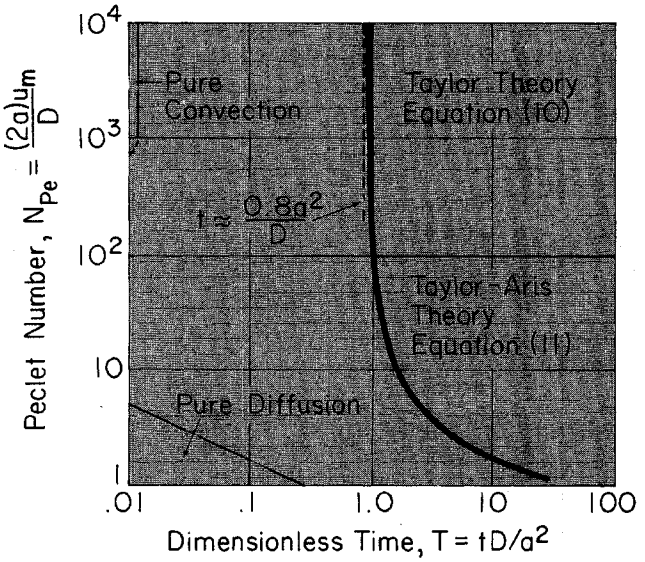

Figure 2. Summary of the regions of applicability of various analytical solutions for dispersion in capillary tubes with a step change in inlet concentration as a function of τ and N_{Pe} (1)

Table I. Minimum Dimensionless Time Required for Taylor-Aris Theory to Apply to Dispersion in a Tube as a Function of Inlet Boundary Condition and N_{Pe} (30)

	τ_{min}		
N_{Pe}	(a)	(b)	(c)
1000	0.80	0.80	0.80
25	1.25	1.25	1.25
10	1.75	0.50	0.50
1	>4.50	4.50	>4.50

There is no equivalent axial dispersion coefficient that can be calculated from these mixing lengths unless the dispersion model region has been reached. Only then can the complete average concentration distribution be computed from a minimum of data.

Effect of inlet boundary condition. The extent to which the nature of the inlet boundary condition influences dispersion was investigated by Gill and Ananthakrishnan (*30*) using finite difference solutions to the convective-diffusion equation for laminar flow in tubes. They considered (*a*) the step change at the inlet ($x = 0$), (*b*) a step change at $x = -\infty$, and (*c*) the Danckwerts' boundary condition at the inlet. The step change at $-\infty$ is exact when two identical infinitely long capillaries, one filled with A and the other with B, are joined at $x = 0$ and the flow is started simultaneously. Danckwerts' boundary condition is an approximation to this situation. The important conclusions reached may be summarized as: (1) for $N_{Pe} > 100$, the dispersion is essentially independent of the inlet condition and (2) for low N_{Pe}, the Taylor-Aris theory applies over significantly larger ranges of the dimensionless time for (*b*) than for (*a*). This last conclusion is significant for small Peclet number experiments if the results are to be interpreted by a dispersion model, since inlet condition (*b*) should be simulated. Table I gives the minimum time for case (*b*) to follow the Taylor-Aris result as a function of the Peclet number.

Slug stimulus. The slug stimulus is an interesting case for study since stimulus response techniques are widely used for determining the flow characteristics of process equipment including porous media. A summary of the work done in this area is available (*44*). Since in real systems a true pulse is difficult to achieve, finite slugs are more generally the case. The main result of

Table II. Minimum Dimensionless Time Required for Dispersion in a Tube with Slug Stimulus to Follow Taylor-Aris Theory as a Function of N_{Pe} (30)

N_{Pe}	τ_{min}
>100	0.60
25	0.50
10	0.30

a finite difference treatment of this problem (*30*) is that the time required for a dispersion model of the Taylor-Aris type to apply is less than that for inlet condition (*b*) above, as is clear if the results summarized in Table II for the slug stimulus are compared with those in Table I. Within the ranges studied, the slug length had little effect on the minimum time requirement, but since condition (*b*) represents an infinitely long slug, and since the results for this case differed from those obtained from the set of small slugs studied, the slug length will have some influence as it becomes longer. For the slug stimulus an approximate criterion for the time required for the dispersion model to apply is

$$\tau_{\min} \simeq \frac{0.6\ N_{Pe}^2}{N_{Pe}^2 + 192}$$

Developing velocity fields and pulsating flow. Two types of problems have been investigated by finite difference solutions of the convective diffusion equation for determining the effects of developing velocity fields on dispersion in tubes (*32*). These include the velocity entrance region wherein the velocity distribution depends on axial distance and the velocity distribution which develops from rest and therefore depends on time. Each of these problems is most likely to be significant in gaseous systems with small Schmidt numbers. For high Schmidt number systems, the velocity entrance region comprises only a small portion of the mixed zone between displacing and resident fluids, and therefore this region is relatively unimportant even at small dimensionless times. For small Schmidt number systems, a relatively large time is required to reach a mixed length equivalent to the velocity entrance length. For velocities developing from rest, the dimensionless time required to reach the fully developed state is inversely proportional to the Schmidt number, such that the time-dependent nature of the velocity is unimportant except for small Schmidt number systems.

In performing experiments, the velocity entrance region would most often be important for the step-change inlet condition while velocity fields developing from rest are more likely to occur in slug stimulus experiments since it is difficult to introduce a well-defined slug of tracer into a flowing stream.

The analytical procedure involving the dispersion model and Equation 12 was also used to study these two situations, so that the applicability of the dispersion model might be determined. For time-dependent velocities, one obtains a dispersion coefficient which is time-dependent (only because the velocity is time-dependent) and the concentration distributions predicted compare favorably with the finite difference results. However, the approach fails for the velocity entrance region (*32*) because of the axial dependence of the velocity which causes the dispersion coefficient to depend on x, in contradiction to the assumption given in Equation 13—*i.e.*, the dispersion model given by Equation 9 is valid only when the velocity does not depend on x. This conclusion was also reached by a different approach by Batchelor (*9*).

The finite difference results, for dispersion with a velocity entrance region, again produced a mean concentration described by an error function at high times. However, the apparent dispersion coefficient determined from this behavior is an unpredictable function of dimensionless time and approached the fully developed value only at large dimensionless times. The apparent dispersion coefficients for this case are smaller than those for fully developed flow. This occurs because the velocity profile is flatter in entrance region flows.

The dispersion coefficient for flows developing from rest is also significantly smaller than the steady-state value and approaches the steady value asymptotically. However, practical use of the dispersion model for this case is possible because error function behavior of the mean concentration is achieved in the finite difference experiments at dimensionless times of approximately 0.6 for large Peclet numbers, which is in close agreement with the minimum time (*1*) required for the dispersion model to apply in steady-state flows.

The effect of the developing velocity field on the extent of dispersion in each case was a decrease in the extent of dispersion. This occurs because nonuniformities in the velocity field in a cross section are greatest when the flow is fully developed.

Aris (*5*), again using the method of moments, investigated the dispersion problem in a tube due to a pulsating pressure gradient in laminar flow. After averaging over one complete period, it was found that if the fluctuations in the pressure gradient are smaller than the mean pressure gradient, the effect of the periodic flow will contribute less than 1% of the total dispersion in the dispersion model regime.

Transition and turbulent flow dispersion. Fortunately, the one-dimensional unsteady dispersion model is more generally applicable to turbulent than laminar flows—*i.e.*, the time required for this model to describe turbulent systems accurately is much less than it is in laminar systems. However, to predict the dispersion coefficient for turbulent flow requires the use of an expression for the velocity distribution and the eddy diffusivity of mass, ϵ_D, which is usually taken to be equal to the eddy diffusivity of momentum, ϵ_m—*i.e.*, since the shear stress, τ_s, is given by

$$\tau_s = -(\nu + \epsilon_M)\rho\frac{\partial u}{\partial r}$$

and the mass flux, n, is given by

$$n = -(D + \epsilon_D)\frac{\partial C}{\partial r}$$

it follows that

$$\epsilon_M = \epsilon_D = \frac{-\tau_s}{\rho\dfrac{\partial u}{\partial r}} - \nu = \frac{-n}{\dfrac{\partial c}{\partial r}} - D$$

if one accepts the Reynolds analogy that $\epsilon_D = \epsilon_M$. This is useful since a great deal more empirical information is available in the literature regarding ϵ_M than ϵ_D. On this basis, the behavior of ϵ_D is known to a reasonable approximation and therefore one can use this expression

for n, together with Equation 1, to describe the concentration distribution.

Once the velocity distribution and eddy diffusivity functions are known, one can proceed to determine the dispersion coefficient for turbulent flow in essentially the same way as for laminar flow—*i.e.*, one uses Equation 6 with D replaced by $D + \epsilon_D$, together with Equations 9 and 12. After Equations 9 and 12 are substituted into the modified form of Equation 6 and one collects coefficients of $\partial C_m/\partial x_1$, the significant part of the f_1 function is given by

$$\frac{1}{y}\frac{d}{dy}\, y \left(1 + \frac{\epsilon_D}{D}\right)\frac{df_{1s}}{dy} = \frac{u}{u_m} - 1 \tag{16}$$

and the boundary conditions for f_{1s}, the steady-state part of the f_1 function, are

$$\frac{df_{1s}}{dy}(0) = \frac{df_{1s}}{dy}(1) = 0 \tag{17}$$

so that f_{1s} is given by

$$f_{1s} = f_{1s}(0) + \int_0^y \frac{1}{\xi\left(1 + \frac{\epsilon_D}{D}\right)} \int_0^\xi \sigma\left[\frac{u(\sigma)}{u_m} - 1\right] d\sigma d\xi \tag{18}$$

with

$$f_{1s}(0) = -2\int_0^y y \int_0^y \frac{1}{\xi\left(1 + \frac{\epsilon_D}{D}\right)} \int_0^\xi \sigma\left[\frac{u(\sigma)}{u_m} - 1\right] d\sigma d\xi dy \tag{19}$$

The expression for the dispersion coefficient, neglecting axial molecular or turbulent diffusion, is then

$$k = -\frac{2u_m{}^2a^2}{D}\int_0^1 y\left[\frac{u}{u_m} - 1\right] f_{1s} dy \tag{20}$$

where

u_m = mean velocity
a = tube radius
D = molecular diffusion coefficient

By assuming $\epsilon_D \gg D$, which is true except very close to the wall, Taylor was able to obtain the very simple expression for k,

$$k = 10.1\, av^* \tag{21}$$

where v^* is the friction velocity defined by

$$\tau_w = \rho v^{*2} \tag{22}$$

This can be related to the Reynolds number through the friction factor, λ, by

$$v^* = \sqrt{\frac{\tau_w}{\rho}} = \sqrt{\frac{\lambda\left(\frac{1}{2}\rho u_m{}^2\right)}{\rho}} = u_m\sqrt{\lambda/2} \tag{23}$$

Consequently

$$k = 7.14\, au_m\sqrt{\lambda} \tag{24}$$

and a variety of formulas are available which express the friction factor as a function of Reynolds number. Presumably Equation 24 is valid for rough as well as smooth pipes.

This result was supported with limited experimental data. However, Taylor used an expression for the velocity profile valid only for fully developed turbulence and did not include axial molecular diffusion since he was concerned with high Peclet number systems. As pointed out later by Tichacek *et al.* (*72*), the accuracy of the predicted dispersion coefficient is very sensitive to the accuracy of the velocity distribution. At a Reynolds number of 42,000, two sets of experimental data for the velocity distribution were employed to compute the dispersion coefficient and, although the the maximum deviation between the two was about 3%, the resulting dispersion coefficients differed by 50%. Tichacek *et al.* finally used the smoothed data of several studies to investigate the dispersion behavior. The difference in the results due to the assumed form of the velocity distribution is again evident in the work of Flint and Eisenklam (*27*) who used other smoothed data and compared their result with the previous theories. Both of these later papers noted that the coefficient in Equation 21 cannot remain constant over the entire turbulent regime from the onset of turbulence.

The interpretation of experimental data for dispersion in turbulent flow has broken down into studies of liquid systems with high Schmidt numbers and gaseous systems with Schmidt numbers near unity. The reason for this, as put forward by Tichacek *et al.*, is that in computing the dispersion coefficient, the changes brought about in gaseous systems by having the Schmidt number different from unity are so small as to be within the error involved in determining the coefficient experimentally. Since the total effective radial diffusion coefficient (using the analogy with momentum transfer) may be written as,

$$\epsilon_D + D = -\frac{\tau_s}{\rho\partial u/\partial r} - \nu\left(1 - \frac{1}{N_{Sc}}\right) \tag{25}$$

assuming the Schmidt number N_{Sc} to be unity, eliminates a term from the expression and the Schmidt number as a parameter. Hence, available experimental data for turbulent flow were correlated separately for gases and liquids. Although Flint and Eisenklam retained the Schmidt number as a parameter, they compared and correlated their own data and theoretical expression only with previous data on gaseous systems. These two papers summarize most of the existing data on turbulent flow dispersion although recent results are reported in (*62A*) and some other interesting results (*70, 71*) will be described in connection with the effects of flow pulsations on dispersion.

The data of Flint and Eisenklam for gaseous horizontal dispersion with a pulse tracer are of interest because they bridge the gap between laminar and turbulent flow in the Reynolds number range 3×10^2 to 10^4 with Schmidt numbers between 0.27 and 1.0. The characteristic shape of a plot of the dispersion coefficient *vs.* the Reynolds number as given by these authors is shown in Figure 3 along with the theoretical result. This is instructive since it demonstrates the effect of turbulence on the dispersion process. [The plot of laminar flow results

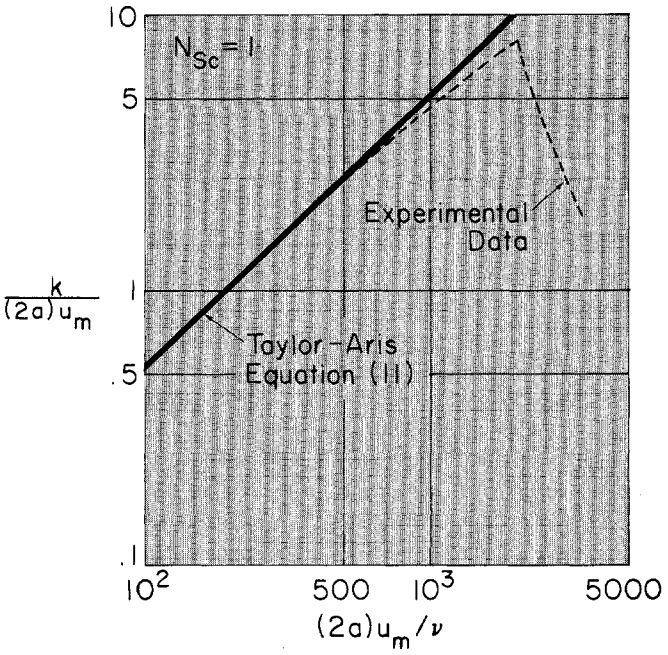

Figure 3. Schematic representation of the effect of transition from laminar to turbulent flow on k. Data in the transition region are available (27)

in Figure 3 as used by Flint and Eisenklam is misleading since it implies that the dispersion coefficient for laminar flow is dependent on the Schmidt number, even though in their experiments the contribution of molecular diffusion was less than 1% (smallest Peclet number about 81). In this situation Equation 33 indicates that the proper dimensionless coefficient is a constant. Although Flint and Eisenklam report deviations from the Taylor result at values of the Reynolds number considerably below the critical value, these deviations do not indicate a discrepancy in the basic theory since they are ascribed to the formation of turbulent spots. Furthermore, the discrepancies occur at different Reynolds numbers for different Schmidt numbers and do not seem to occur to any considerable degree at a Schmidt number of 0.27 (see their Figure 6).]

Over the range of Reynolds numbers 10^2 to 10^3 the experimental data follow the Taylor results and peak at approximately the critical Reynolds number followed by a rapid decrease as the Reynolds number increases further. In turbulent flow as compared to laminar, material is dispersed by the additional mechanism of eddy diffusion. In the radial direction, this enhances the action of radial molecular diffusion and hence the dispersion coefficient decreases. Tichacek *et al.* and Taylor have presented arguments which indicate that turbulent axial diffusion has negligible effects on the dispersion because its contribution is small compared to mixing caused by radial differences in the velocity.

Axial dispersion in concentric annuli in fully developed turbulent flow was studied by Smith (*65*) both experimentally and with a Taylor dispersion model. Again, an extreme sensitivity of the predicted dispersion coefficient to the velocity distribution used was noted. Experimental results for pipes and annuli correlated well if the hydraulic diameter was used as the length parameter.

Unsteady turbulent flow due to a sinuosidal pressure gradient in a liquid system was studied experimentally by Taylor and Leonard. Although the initial results (*70*) indicated a large increase in the dispersion due to small amplitude pulsations, later experiments (*71*) failed to reproduce the initial results and demonstrated only small changes in the dispersion coefficient due to small flow pulsations. An analytical treatment of this problem is now in progress (*47*), and preliminary results indicate that the trends of the experimental findings may be predicted using an empirical eddy diffusivity in the dispersion model.

Interesting steady turbulent flow dispersion results

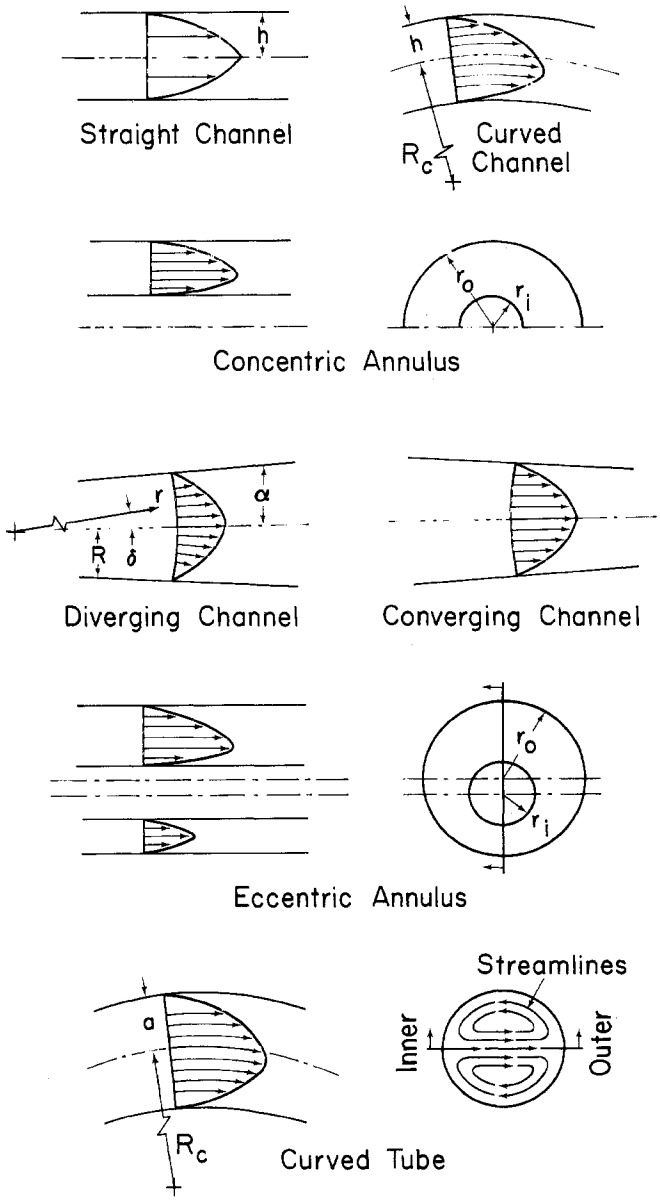

Figure 4. Diagrams of various microstructure units indicating the nature of the velocity profiles

on a liquid system are reported by Taylor (*71*) for comparison with the pulsating flow result. Two different tube sizes of commercially "drawn" tubing were used in experiments over a Reynolds number range of 3500 to 26,000, namely 0.242 in. and 0.745 in. i.d. For the larger tube, the results are in reasonably good agreement with the correlation suggested by Tichacek *et al.* For the smaller tube, the results are significantly higher (by about a factor of 2). One explanation for this may be the tube roughness. On the assumption that the two tubes had the same size roughness elements, it is possible that the roughness affected the results in the small tube but not in the large one. The friction factor in Equation 24 is a function of only the Reynolds number if the tube is hydraulically smooth. If, however, the roughness elements are large enough so that the system cannot be considered smooth, then λ increases as the relative roughness, the ratio of the height of a roughness element to the tube radius, increases. Hence, Equation 24 predicts trends in agreement with the experimental results if the small tube is assumed to have a larger relative roughness than the larger tube. As noted by Tichacek *et al.*, roughness tends to make the velocity less like plug flow than in systems which may be considered hydraulically smooth, and hence increases the dispersion. However, studies of the friction factor variation with Reynolds number by Taylor failed to show any significant dependence on tube size.

Other Microstructure Units

A number of microstructure units other than straight capillary tubes are of interest in formulating a description of possible geometries making up the macrostructure. Among those which have significant effects on the nature of the dispersion and which have been investigated using either the finite difference solution of the convective diffusion equation and/or the dispersion model procedure are: (1) the straight channel; (2) the straight annulus, both concentric and eccentric, wherein the effects of an asymmetrical velocity profile may be isolated; (3) the curved channel and tube which introduce the effect of curvature and secondary flow in the tube case; and (4) converging and diverging channels which have the important property of nonparallel boundaries. A schematic representation of the various units is given in Figure 4. In addition, the mixing cell may form one of the important units in the microstructure, and a series of stirred tank arrangements is frequently used in the literature (*43*, *50*, *75*) as a model of porous media.

It is important to investigate the relationship between the mixing cell model and an actual porous medium to determine if such a model is physically realistic in the ranges of flow rates over which it has been used. The correlation of much of the experimental data existing in the literature for unconsolidated media, such as sand packs by Perkins and Johnston (*50*), demonstrates that an effective axial dispersion coefficient correlates well with the first power of the mean interstitial velocity over a fairly large range of velocity, although to cover very large ranges of velocity a power series in a Peclet number based on pore dimensions (*39*) may be required. The mixing cell model can be used to predict that the dispersion coefficient is proportional to the velocity whereas in a single capillary, the dispersion coefficient is proportional to the square of the velocity. However, the mechanism which one would consider as forming a mixing cell at the junctures of solid particles—*i.e.*, turbulent mixing—has not been observed in such media and furthermore—if the velocity is increased, experimental dispersion coefficients become proportional to a higher power of the velocity. Visual observations by von Rosenberg (*78*) and Blackwell (*11*) suggest that individual streams retain their identity at a juncture in a sand pack and that transport occurs between them solely by molecular diffusion. Hence, the mixing cell in this case really approximates a situation which occurs at relatively low flow rates such that the fluid streams from different pores leading to a juncture remain in the junction sufficiently long enough to have their concentrations equalized by molecular diffusion and not turbulent mixing. The situation is different in other types of packing. For example, Shulman and Mellish (*62*) observed the flow patterns in a column packed with 1-in. Raschig rings and found that although laminar flow predominated in the flow over packing, turbulent mixing occurred at the junctions between pieces of packing.

Straight channel. The dispersion coefficient for a parallel plate duct with fully developed laminar flow can be shown to be (*54*, *74*):

$$k_{f.p.} = D + \frac{8}{945}\frac{u_{\max}{}^2 h^2}{D} \tag{26}$$

where h is the half-width of the channel and $u_{\max}$ is the centerline velocity. Subject to a step change in inlet concentration, the mean concentration in the region of applicability of the dispersion model is

$$C_m/C_0 = 1/2\left\{\operatorname{erfc}\left(\frac{x_1}{2\sqrt{k_{f.p.}}}\right) + \exp\left[\frac{u_m(x_1 + u_m t)}{k_{f.p.}}\right]\operatorname{erfc}\left(\frac{x_1 + 2u_m t}{2\sqrt{k_{f.p.}\,t}}\right)\right\} \tag{27}$$

The full convective diffusion equation has been solved by finite difference (*33*) and the regions of validity of analytical solutions are shown in Figure 5. Note that for the dispersion model to apply requires a dimensionless time $\tau = tD/h^2$ of approximately unity. At high Peclet numbers with the same fluids, a straight channel having the same equivalent diameter (four times the hydraulic radius) as a tube requires a minimum real time of approximately 1/3 of that for the tube before the dispersion model applies, thus indicating that the minimum real time requirement is a strong function of the geometry of the system.

Concentric and eccentric annuli. The concentric annulus represents a generalization of the straight channel and straight tube cases and demonstrates the effect of an asymmetric velocity distribution of dispersion. The dispersion coefficient for this situation (*33*) is a

function of the radius ratio, $1/\kappa$, the ratio of outside to inside radii, r_o/r_i. For small values of $1/\kappa$ (narrow gap) ≤ 1.5, the flat plate result given in Equation 26 may be written as

$$k = D + \frac{8}{945}\left[\frac{r_o^2 u_{max}^2(1 - \kappa^2)}{4D}\right] \qquad (28)$$

with r_o the radius of the outer cylinder; it provides an excellent approximation to the annulus result. As the radius ratio increases, the dispersion coefficient becomes larger than predicted by Equation 28, thus indicating that the effect of an asymmetrical velocity is to increase the dispersion relative to the symmetrical case of the straight channel. As $1/\kappa$ approaches 100, the dispersion coefficient approaches that for a tube given in Equation 11. The limits of applicability of the dispersion model with respect to time have not yet been established but for the limiting cases (and probably in between), they may be inferred from the results for tubes and channels given previously.

Dispersion in eccentric annuli is most markedly affected by the degree of eccentricity when the ratio of the outer to inner radius approaches unity so that the system approximates nonparallel plates with a constant cross-sectional area along the direction of flow (*60*). Over the range of radius ratios and eccentricities studied, the dispersion coefficient can vary by more than two orders of magnitude with changes in eccentricity.

Curved systems. The curved tube with fully developed laminar flow has the additional complicating factor of a secondary circulatory motion in a cross section superimposed on an asymmetrical axial velocity profile. Jones (*40B*) and Wright (*81*) have recently presented evidence that such circulations are the reason for departures from Darcy's law in granular beds. For large values of the ratio of the radius of curvature to the tube radius RC/a, Erdogan and Chatwin (*25*), using an approach similar to Taylor's (*67*), demonstrated that the effect of curvature is to decrease the dispersion coefficient over that in a straight tube if the Schmidt number is >0.124. Later it was demonstrated (*46*), by relaxing the assumption with regard to curvature ratio, that the competing effects of transverse mixing caused by the secondary flow and the asymmetrical axial velocity cause the dispersion coefficient first to increase above and then decrease below the straight tube result as the Reynolds number increases, these effects being most pronounced at small values of the curvature ratio. The applicability of the result with respect to the minimum time requirement is not yet available although approximate minimum times have been estimated (*47A*).

In the curved channel, no secondary flow exists and hence the dispersion coefficient is increased over that in a straight channel under the same conditions. The effect of molecular diffusion on dispersion is modified by the curvature. For example, in the curved channel, for a given Peclet number, molecular diffusion contributes a smaller fraction of the total dispersion effect than it does in straight channels.

Experimental studies on miscible displacements in

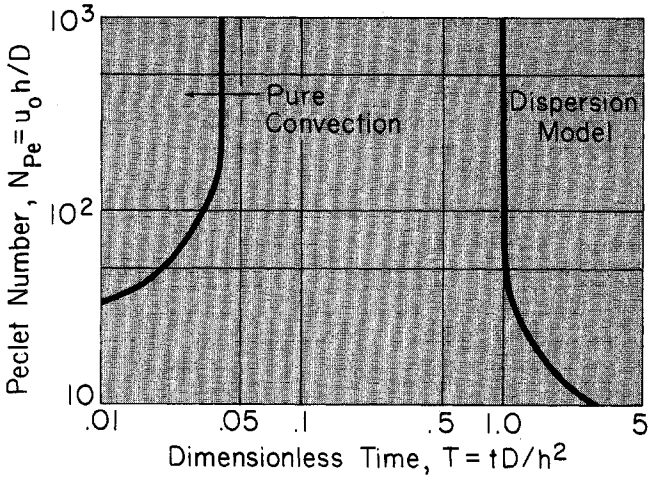

Figure 5. Summary of the regions of applicability of analytical solutions for dispersion in straight channels with a step change in inlet concentration as a function of τ and N_{Pe} (33)

systems with curvature have mainly involved turbulent flow, and conflicting results concerning the effect on the dispersion have been reported (*6*, *16*, *17*, *41*). These discrepancies may be due to differences in the experimental apparatus used or to differences in the turbulence characteristics of the flow, but it appears that more work is needed in this area.

Converging and diverging channels. Flow in the interstices of porous media experiences local accelerations and decelerations because of changes in cross-sectional area. Some indication of the effect of variable area passages on the dispersion process has been provided by a recent study of Jeffrey-Hamel flows between nonparallel flat planes (*33*, *36*). Even small angles of divergence can markedly affect the dispersion process, particularly when the Peclet number is large. Perhaps the most striking result of this study is that the pure convection solution is valid for dispersion in flow between nonparallel walls for much larger values of dimensionless time than for parallel plate or capillary systems. The implication is that both transverse and axial molecular diffusion play a minor role in dispersion in diverging channels at high Peclet number.

Some physical insight into the reasons why molecular diffusion is less effective can be gained by considering the velocity distribution. For stable, fully developed flow in diverging channels the velocity field can be written in terms of Jacobian elliptic functions which can be simplified considerably for small Reynolds numbers and angles of divergence to the form

$$u = \frac{U_{ent} R}{\tan \alpha}\left(\frac{1}{r}\right)(1 - \theta^2)$$

where

U_{ent} = velocity at entrance to system
R = halfspacing at entrance to system
α = angle of divergence
r = axial coordinate
θ = dimensionless angular coordinate (δ/α)

If one plots this distribution, it becomes flatter as one moves downstream. This reduces the surface area across which a steep radial concentration exists, compared to that in parallel plates, and therefore decreases the effect of transverse molecular diffusion. As the velocity gets flatter, in the limit, the surface area across which molecular diffusion occurs degenerates to a plane, the outer normal of which is parallel to the direction of main flow. In contrast, with tubes or parallel plates the velocity profile is invariant with axial position and as time increases, convection creates an increasingly large paraboloid surface, across which transverse concentration gradients are very large.

Capacitance Effect

The existence of stagnant pockets of fluid in porous media due to dead-end passages along the flow path is one consequence of the geometry of the medium which may be incorporated relatively easily into the microstructure capillary model. The effect of system capacitance is to increase the length of the mixing zone. Capacitance models for porous media have been suggested and employed for the interpretation of experiments by several authors (*18*, *21*, *34*, *37*, *38*, *45*, *50*, *73*, *74*). To construct the microstructure model, some physical picture of the nature of the stagnant regions must be assumed. One extreme of the types of stagnant regions possible is the "bottleneck" (*18*, *34*) shown in Figure 6*a* wherein the concentration of the main volume of stagnant fluid is assumed to change with time, due to a steady-state diffusion process in the pores leading to the main volume. Turner (*73*) visualized a porous medium as consisting of rectangular dead-end pockets communicating with the main flow channels as shown in Figure 6*b*. Material passes into or out of these pockets only by molecular diffusion. In the main channels, dispersion takes place by convection and diffusion, while the concentration in the stagnant volume changes according to

$$\frac{\partial C}{\partial t} = D\frac{\partial^2 C}{\partial y^2} \tag{29}$$

Later Gill and Ananthakrishnan (*30*) used a continuous stagnant pocket or Turner structure as shown in Figure 6*c*. The point concentration in the stagnant region varies according to the two-dimensional unsteady diffusion equation. The continuous Turner structure retains the elements of the other representations and is simplest to deal with numerically. Hence, we shall consider in some detail the analysis and results for the Turner model microstructure unit.

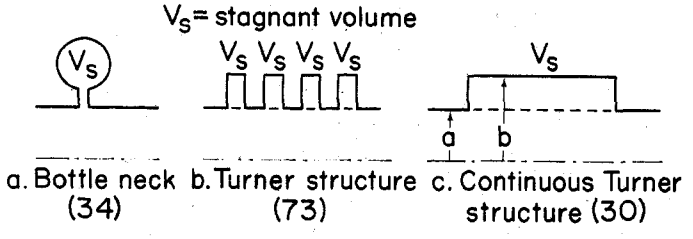

Figure 6. Diagrams of different capacitance models

Turner (*73*) and later Aris (*2*), who generalized the Turner model, were concerned with the frequency response of such models and did not discuss the applicability of a dispersion model, although Turner (*74*) interpreted some experimental results for a flat plate system to which were connected dead-end capillaries by using a Taylor dispersion coefficient based on the distance between plates. However, Aris (*3*) pointed out that the Taylor-Aris result given in Equation 11 is not the correct expression for the dispersion coefficient in Turner-type structures. Using the method of moments it was determined that the Taylor dispersion coefficient could be anywhere from one to 11 times the value it has for a straight capillary without the capacitance effect. The low and high extremes occur when there are no stagnant regions and when the ratio of stagnant volume to pore volume become infinite, respectively.

The applicability of a dispersion model of the type postulated in the Taylor-Aris theory was investigated with numerical experiments by Gill and Ananthakrishnan (*30*) on the continuous Turner structure for various inlet boundary conditions, Peclet numbers and stagnant to pore-volume ratios. For high Peclet numbers ($N_{Pe} \gtrsim 100$) where the effects of inlet boundary conditions and axial molecular diffusion are unimportant, the mean concentration becomes an error function at sufficiently high dimensionless time. A comparison of the result given in Equation 30

$$C_m/C_0 = 0.5\left[1 - \operatorname{erf}\left\{\frac{x - u_{max}t/2\gamma^2}{\sqrt{4kt/\gamma^2}}\right\}\right] \tag{30}$$

where γ is the ratio b/a in Figure 6*c*, with the Taylor theory demonstrates that dispersion in Turner structures must be considered to take place in a tube of sufficient radius to include the stagnant pore volume rather than just the main channel volume alone; then the dispersion coefficient obtained by Aris (*3*)

$$k = \left[\frac{8(1+\beta) + 12(1+\beta)^2 \ln(1+\beta) - 7(1+\beta)^2}{(1+\beta)^2}\right] \times \frac{u_{max}^2 a^2}{192D} \tag{31}$$

where $\beta = \gamma^2 - 1$

Table III. Minimum Values of Dimensionless Time Necessary for Dispersion Model to Apply to Continuous Turner Structure Capacitance Model at $N_{Pe} \geq 100$ as a Function of Ratio, Total Volume to Pore Volume, γ (30)

γ	τ_{min}
1.0	0.80
1.1	1.25
1.2	2.00
1.3	4.00
2.0	>15.00

can be used to predict the mean concentration. This result implies that for complex systems, such as porous media, the entire void volume should be used in determining flow parameters.

The numerical experiments (*30*) demonstrated that for high Peclet number systems, the limiting value of the dimensionless time necessary for Equations 30 and 31 to predict the mean concentration distribution was a function of γ as shown in Table III. It is clear from Table III that systems having a large capacitance require significantly longer times before a dispersion model applies. This implies that for porous media with large amounts of dead space a long length is required to ensure sufficient residence time for the effluent concentration to obey the error function description.

For low values of the Peclet number, the effects of axial molecular diffusion and inlet boundary conditions create a more complex situation. At very low Peclet numbers, pure molecular diffusion is the controlling mechanism if

$$N_{\mathrm{Pe}}\sqrt{\tau}\begin{cases}<0.4 \text{ with } \gamma = 1.2\\ <0.5 \text{ with } \gamma = 1.0\end{cases} \qquad (32)$$

For large values of the dimensionless time, the mean concentration again becomes an error function; however, in this situation, the minimum time is strongly dependent on Peclet number and the nature of the inlet boundary condition. Interestingly, the trend of behavior is not the same as that for tubes without capacitance for inlet conditions of the types *b* and *c* described previously. In fact, the minimum time required for case *b* to be described by an error function, as given in Table IV, is reduced from 2.75 to 1.0 by changing the Peclet number from 25 to 10. Note that this lower value is less than that required at high Peclet numbers. The minimum values of time listed in Table IV reinforce the conclusion drawn previously that if miscible displacements are to be interpreted by using a dispersion model they should simulate inlet boundary condition *b* since this will reduce markedly the system length necessary.

It is significant to note that using an analysis similar to that used originally by Taylor (*67*, *69*), Gill and Ananthakrishnan were able to predict local concentration distributions which agreed with the finite difference experiments at sufficiently large values of time using the entire void volume of the system. This implies that local as well as average behavior may be predicted in complex systems if only the local velocity distribution is known.

Dayan and Levenspiel (*20A*) further generalized the Turner model to include adsorption on the solid surface including that inside the dead end pores. Thus they were able to simulate the separate effects of holdup in the pores and adsorption on the surface. They employed the method of moments developed by Aris. For the case of a linear equilibrium relation between phases and assuming equilibrium always exists between the interfacial liquid and the adsorbed phase, they derived an expression for the dispersion coefficient and showed that adsorption increases the dispersion coefficient. Furthermore they showed that pore holdup and adsorption are not simply additive contributions to the dispersion coefficient but are combined in a complex fashion.

Aris (*4A*) also applied his moment analysis to the case of two phases flowing contiguously with heat or mass transfer across the interface between them. This interesting analysis provides the basis for analyzing both cocurrent and countercurrent systems. Gill (*33A*) using a generalized version of the series expansion in Equation 12, later extended the two phase problem to include the effect of time variable flow. The dispersion coefficient obtained from these analyses should be used in conjunction with a dispersion model based on the average velocity for the entire system (*33A*).

Buoyancy Effects in Tubes

From a dimensional analysis of the general equations of change for dispersion in tubes, it is possible to demonstrate that the dispersion process depends on the independent parameters

$$N_{\mathrm{Pe}} = \frac{au_m}{D},\ N_{\mathrm{Re}} = \frac{au_m\rho_0}{\mu_0},\ N_{\mathrm{Gr}} = \frac{a^3g(\Delta\rho/\rho_0)}{\nu_0^2},\ N_{\mathrm{Fr}} = \frac{u_m^2}{ag}$$

these being, respectively, the Peclet, Reynolds, Grashof, and Froude numbers. Thus far we have considered laminar systems in which density and viscosity differences between resident and invading fluids are negligible and no free surface exists. Hence, it is easily demonstrated from Equation 11 for straight capillary tubes that the dimensionless dispersion coefficient, K, depends only on the Peclet number, and for large N_{Pe}, K is independent of the Peclet number.

$$K = \frac{k}{DN_{\mathrm{Pe}}^2} = \frac{1}{N_{\mathrm{Pe}}^2} + \frac{1}{48} \qquad (33)$$

In practice, density and viscosity differences give rise to significant changes in the nature of dispersion in both capillary tubes and porous media. In a completely submerged system in which density is constant, the effect of gravitational force is eliminated by the proper choice of static pressure and hence, the Froude number which represents the ratio of inertial to gravitational forces is not a parameter. In displacement systems with density differences, however, it is not immediately evident that the initial interface established between resident and invading phases does not have some of the properties of a free surface. Surface tension–driven convection can also play a role in determining the nature of the process which occurs at this interface. Some of the effects which arise in horizontal and vertical

Table IV. Minimum Values of Dimensionless Time Necessary for Dispersion Model to Apply to Continuous Turner Structure Capacitance Model as Function of N_{Pe} with $\gamma = 1.2$ (*30*)

N_{Pe}	τ_{min}
1000	2.00
25	2.75
10	1.00

systems due to natural convection caused by concentration gradients are considered here.

A number of studies of miscible displacements in tubes (*13*, *26*, *55*, *56*, *67*, *76*) have verified the Taylor theory for large Peclet numbers and dimensionless times near or greater than unity. A majority of these results are for systems wherein the two fluids have approximately the same density and viscosity. More difficulty has been experienced with experimental verification of the Aris modification for small Peclet numbers, although the work with gases of Evans and Kenney (*26*) for large values of the dimensionless time and the experiments with liquids of Rejhsinghani *et al.* (*56*) for small values of time and small bore tubes show excellent agreement when effects not included in the Taylor-Aris theory are not present. The main factor associated with deviations from this theory at low values of the Peclet number appears to be natural convection currents established by concentration gradients, although instabilities in the flow may contribute.

Significant deviations from the Taylor-Aris result for higher times and from the numerical experiments (*1*) at lower times have been noted in horizontal systems with density differences $\Delta\rho/\rho$ as small as 1.2×10^{-4} in aqueous solutions (*56*). Bournia *et al.* (*13*), working with gases having the same molecular weight in vertical downward flow, found large discrepancies between theory and experiment in the low Peclet number range. Density differences in such gaseous pairs are due to differences in the compressibility factors. It has been estimated (*56*) that the Grashof number for their experiments was on the order of magnitude of 10,000, thus indicating that natural convection effects were probably present.

From first considerations, natural convection seems to have a different influence on the extent of dispersion in horizontal and vertical systems since, in the first, the action of gravity is normal to the main flow and, in the second, parallel. We shall now explore the modes by which natural convection influences the dispersion.

Assuming a step change in the inlet concentration at time zero, at small values of time, axial convection dominates and a parabolic finger of the displacing fluid invades the resident fluid. This situation prevails in both horizontal and vertical systems and whether the light fluid displaces the heavier or vice versa.

In horizontal systems, if the heavier fluid displaces the lighter, at low flow rates, the core of heavier fluid tends to sink to the tube wall displacing the less dense fluid and creating a transverse movement in the cross section. If the lighter fluid is used as the displacing medium, the core tends to rise, again creating a transverse motion. This secondary movement increases radial mixing—*i.e.*, it enhances the action of radial molecular diffusion and thus tends to inhibit axial dispersion. However, there is a second effect in systems with natural convection which must be considered.

Axial density gradients cause a variation in the axial pressure gradient and thus axial movement. For the case of a denser fluid displacing a lighter one, this effect enhances axial movement in the flow direction, thus enforcing the effects of axial convection and increasing the amount of axial dispersion. These two effects of natural convection in horizontal systems are competitive, one tending to increase and the other to decrease the axial dispersion. The experimental results (*56*) agree with theory which predicts that in the low Peclet number range, natural convection enhances axial dispersion at lower Peclet numbers and depresses it at higher Peclet numbers. For intermediate values, where the two competing effects cancel, and for very large Peclet numbers, where natural convection is negligible, the experimental results approach the numerical solution ignoring natural convection. This was first explained qualitatively on the basis of an analogy to heat transfer (*56*) and later explained quantitatively by the analysis of Erdogan and Chatwin (*25*).

Buoyancy effects in vertical upward displacements can either increase or decrease the extent of axial mixing depending upon whether the heavy or light fluid is the displacing medium. The contributing effects can again be explored if one considers the small time behavior of the system. At small times, a paraboloid of displacing fluid invades the resident fluid as shown in Figure 7*a*. If we ignore the effects of molecular diffusion, as time increases, if the heavy fluid is the displacing fluid, in a cross section, the centrally located fluid is denser than that near the wall, and therefore the action of gravity is to retard the movement near the centerline and accelerate it near the wall. The flattened profile in Figure 7*b* results.

If the heavier phase is displaced, the action of gravity is to accelerate the central core relative to the fluid near the wall, and the elongated profile of Figure 7*c* occurs. Comparison of the relative lengths of the zones over which the invading fluid is present in Figures 7*b* and 7*c* shows that the axial dispersion is depressed by natural convection in case *b* and enhanced in case *c*. An approximate analytical analysis which predicts these trends is given by Reejhsinghani *et al.* (*55*).

When the initial interface is created, if the lighter phase is on the bottom and displaces the heavier one, we have an unstable hydrodynamic system which is analogous to the classical problem of a fluid layer heated from below. This instability has a profound effect on the process as evidenced by the experiments (*55*). In

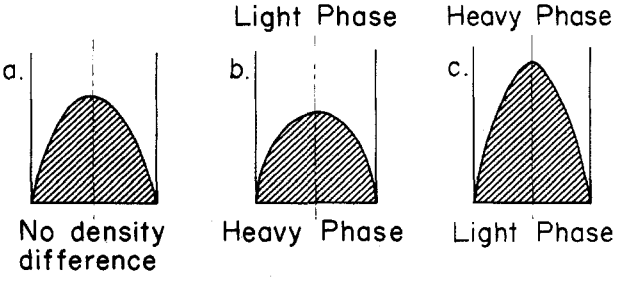

Figure 7. Schematic diagrams illustrating the effect of buoyancy on dispersion in vertical upward displacements in tubes

particular, for such unstable cases, the approximate theory which ignores this effect grossly underestimates the value of the dispersion coefficient.

In downward flow, the same arguments applied to upward flow can be used to predict that a heavier fluid displacing the lighter should lead to increased axial mixing and a lighter displacing the heavier to decreased axial mixing. These mechanisms would seem to apply as long as the system is in stable laminar flow.

The vertical downward experiments of Bournia *et al.* (*13*) are more difficult to interpret since slugs of tracer gas were used rather than the step change in inlet concentration. The small density differences in these experiments were noted previously. Each of the gases was used as the slug with the other as the surrounding medium. Hence, both a light slug in a heavy carrier phase and a heavy slug in a light carrier stream were investigated. The configurations which exist at small times are shown in Figures 8*a* and 8*b*. By the previous arguments, the two slugs will be distorted by gravity into the shapes shown in Figures 8*c* and 8*d*. In the case of the heavy slug, the forward portion is elongated and the rear flattened. If the flow is stable then clearly the mixing length is increased. For the light slug the situation is not clarified by this simple analysis since the rear portion of the slug will tend to catch up with the front portion. The experiments of Bournia *et al.* yielded large increases in the amount of dispersion for both types of experiments at low velocities. In the case of the heavy slug, the trend is predicted by our simple analysis while for the light slug the analysis fails. Perhaps in both cases the stability of the flow should be examined since a heavy fluid on top of a lighter one in a vertical system is an unstable state; clearly, with a slug of different density from its surroundings, one of its two interfaces is always unstable.

Most experimental data available on vertical displacements in porous media have been performed with a favorable density difference—*i.e.*, the less dense fluid above the more dense, since viscosity instabilities are lessened by favorable density gradients, as will be described later. Hence, existing analytical studies of the stability problem have focused mainly on the description of viscous fingering and assumed matched densities or favorable density gradients. It is important to note that gravity effects in porous media even for fluids of apparently matched densities (matched to two significant figures, for example) may have significant effects and, by analogy to capillary tubes, render a dispersion model useless for interpreting results.

Viscosity and Density Effects in Porous Media

Since density effects have been found to influence significantly the nature of dispersion in capillary tubes, it is pertinent to examine the literature pertaining to porous media to determine if similar effects are noted. Viscosity and/or density differences can lead to unstable displacements—*i.e.*, the formation of viscous "fingers" or a gravity "tongue" of displacing fluid in the resident phase. These effects, which are described further below,

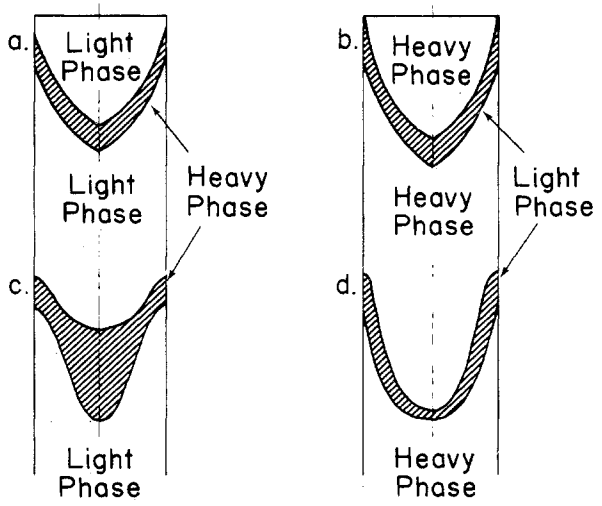

Figure 8. Schematic diagrams illustrating the effect of buoyancy in downward flow with a slug stimulus

tend to lengthen the mixed zone between phases; thus, they have a deleterious effect in most practical miscible displacements. Several different possibilities exist for the interaction of viscosity and density effects. One may have either a favorable viscosity ratio (the displacing fluid is more viscous than the displaced phase), or an unfavorable viscosity ratio coupled with either a favorable (the upper fluid is less dense than the lower in a vertical system), or an unfavorable density difference. Viscosity ratios and density differences are favorable if they result in a shorter mixed zone.

Consider first a system with matched densities. Viscous fingering results if the displacing fluid penetrates at different rates in a cross section of the porous medium. This initial preferential penetration is evidently due to local heterogeneities in the permeability, since it occurs (*12*) in what would normally be considered homogeneous media (*e.g.*, sand packs with a small range of particle size). Under an unfavorable viscosity ratio, these initial fingers grow in length and width with distance penetrated. Such fingers have been observed by several workers (*12*, *39*, *64*) and resemble those shown in Figures 9*a* and *b* for very high and smaller unfavorable viscosity ratios in horizontal systems. At low flow rates, transverse diffusion has been observed (*64*) to cause the formation of one large finger. As indicated in Figure 9, viscous fingering can lead to bypassed regions and extremely long mixed zones as the viscosity ratio becomes more unfavorable. Although this is an extremely complex phenomenon, Peaceman and Rachford (*49*) were able to solve a mathematical model which yielded qualitative behavior similar to that shown in Figure 9. To cause fingers to form spontaneously in the mathematical model, it was necessary to use small random variations of permeability with position. Other mathematical analyses of horizontal systems have been given (*23*, *42*).

Matched density experiments in vertical upward flow with both favorable and unfavorable viscosity ratios have been reported by Brigham *et al.* (*14*). Results

showed: (*a*) for favorable viscosity ratios of 0.175 and 0.998 and unfavorable ratios of 1.002 and 5.71, the mixing zone length increases as the viscosity ratio increases; (*b*) a change from a favorable viscosity ratio of 0.998 to 1.002 unfavorable brought about a disproportionately large increase in the mixing zone length; and (*c*) for unfavorable viscosity ratios, the mean concentration at the outlet did not follow the error function behavior of Equation 4. Point (*b*) has been discussed (*40*) with regard to the prediction of stability theories, while von Rosenberg (*78*) has mentioned an effect similar to that in point (*c*), and the downward flow matched density experiments of Slobod and Thomas (*64*) for unfavorable viscosity ratios do not appear to have the characteristic error function "S" shape on a plot of mean concentration *vs.* pore volumes injected although these data were not plotted on probability paper to test this.

Gravity tonguing occurs in horizontal systems as the less dense displacing phase (most experiments available have used this arrangement) tends to flow over the more dense resident phase, thus increasing the mixing length. Experimental evidence for this effect has been reported (*68, 69, 77*). In slow flows with large gravity effects, the tendency is to form one large finger (*20*) of displacing fluid rather than several smaller fingers. Transverse mixing by molecular diffusion is probably enhanced by natural convection in this situation by a mechanism similar to that described for empty tubes previously, so that the displacement front is smoothed out compared to that shown in Figure 9. Density effects are also considered in mathematical models (*23, 49*).

In vertical systems, gravity effects may be used to inhibit viscous fingering and may effectively prevent the formation of fingers under certain conditions. Consider the schematic diagram in Figure 10 of a vertical downward displacement with a lighter, less viscous fluid invading the resident fluid. If viscous fingering occurs, then the shaded area represents the region occupied by the displacing fluid. A cross-sectional cut of the medium is denoted by the two horizontal lines. In the heavily shaded regions the material is lighter than the unshaded areas because of the density difference. Hence, the action of gravity will be to accelerate flow through the unshaded regions and to retard flow in the shaded regions as indicated by the direction of the arrows. Thus, the gravity effect is clearly one of inhibiting the growth of viscous fingers and reducing the length of the mixed zone. If the positions of the heavy and light fluids are reversed but the unfavorable viscosity ratio is maintained, then the growth of viscous fingers is accelerated by density effects. This reasoning is analogous to that used to explain the effect of gravity on the velocity distribution for displacements in tubes.

Some of the most extensive experimental work on the length of the mixed zone under all four combinations of viscosity and density differences in vertical downward displacements was carried out by Slobod and Howlett (*63*). For a less viscous, less dense displacing phase, a simple stability analysis which assumes no mixed zone

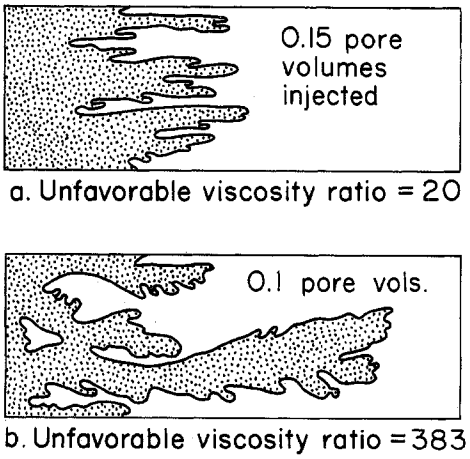

Figure 9. Schematic representation of viscous fingering in a horizontal porous medium for two unfavorable viscosity ratios (12)

and uses Darcy's law with gravity effects included has indicated that a critical flow rate exists below which the displacement is stable (*24, 51–53, 79, 80*). If one considers a horizontal, sharp interface between the two phases in which a small dimple of invading fluid has formed in the resident phase, then if the pressure gradient in the displacing phase is larger than the pressure gradient in the resident phase, this protrusion will grow and the displacement is considered unstable. If the pressure gradient in the displacing phase is less than that in the resident phase, the protrusion is suppressed and the displacement stable. The criterion for stability is thus

$$\left(\frac{dp}{dx}\right)_d < \left(\frac{dp}{dx}\right)_r$$

or using Darcy's law

$$\frac{-q\mu_d}{P} + \rho_d g < \frac{-q\mu_r}{P} + \rho_r g$$

Hence the critical volumetric flow rate is given by

$$q_c = Pg\,\frac{(\rho_r - \rho_d)}{(\mu_r - \mu_d)} \qquad (34)$$

In Equation 34, P is the permeability and the subscripts d and r denote the displacing and resident phases, respectively. The ratio of the experimental flow rate q to the critical q_c was used by Slobod and Howlett to correlate their results for various flow rates, viscosity ratios, and density differences within one class of experiments—*e.g.*, favorable viscosity and density ratios. The ratio q/q_c represents essentially the ratio of viscous to gravity forces or, in dimensionless groups, the ratio of the Reynolds number to the Grashof number.

A summary of the experiments using fluids with no density differences as the reference cases is given in Table V. These results clearly demonstrate that the effect of gravity on the mixing zone length is explained qualitatively by the elementary physical arguments advanced previously. Furthermore, rather large changes in the mixing zone length were affected in the cases where flow rates were small enough for gravity forces to become im-

portant. These effects were most pronounced for unfavorable viscosity ratios but also strongly influenced the mixing zone length for $q/q_2 < 1$ with favorable viscosity ratio but unfavorable density ratio.

Dumore (*24*) offers a treatment of stability based on the same criterion regarding the pressure gradient but assuming monotonic concentration changes in the mixed zone and a monotonic dependence of the density and viscosity on the concetration in the mixed zone. Perrine (*51–53*) has applied the theory of hydrodynamic stability using Darcy's equation as the equation of motion, although some of this work has been questioned (*48*). For more recent and extensive treatments of the stability problem for vertical systems in the presence of viscosity and density differences and including the effects of a mixed zone between resident and displacing fluids, the works of Schowalter (*61A*) and Heller (*40A*) are recommended.

Summary

We have tried to point out how the mechanisms of dispersion in simple geometries reflect on the more complex problem of dispersion in porous media, and in particular we have emphasized the restrictions necessary for a diffusion-type equation—*e.g.*, Equation 3—to describe miscible displacements. The most definitive study of this question is presented by Bischoff and Levenspiel (*10*). By considering the time involved in the process to be approximately the mean residence

Table V. Summary of Effects of Density Differences on Mixing Zone Length in Vertical Downward Displacements in Porous Medium with Both Favorable and Unfavorable Viscosity Ratios (*63*)

Experimental results compared to reference cases with no density differences

Viscosity ratio	Density difference	Comments
Favorable	Favorable	Mixing zone length shows only minor decreases over the reference case
Favorable	Unfavorable	Mixing zone length shows a rapid and large increase as q/q_c becomes <1, indicating viscous fingering. Close agreement with reference case for $q/q_c \geq 2$
Unfavorable	Favorable	Mixing zone length shortened significantly and approaches the reference case as $q/q_c \rightarrow 7$
Unfavorable	Unfavorable	Mixing zone length shows large increases for $q/q_c \geq -3$. The reference case is approached near $q/q_c = -7$

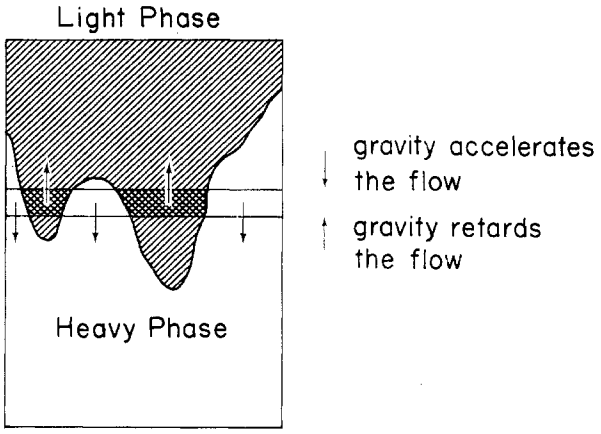

Figure 10. Diagram illustrating the tendency of a favorable density difference to smooth out the displacement front in a porous medium

times, L_T/u_m, where L_T is the length of the system in the main flow direction, these investigators concluded that

$$\frac{L_T}{(2a)} > 0.04\,\frac{(2a)u_m}{D} \qquad (35)$$

was a criterion for the applicability of the dispersion model. By introducing an effective or hydraulic diameter for packed tubes and the particle diameter, this same criterion was used to establish order of magnitude estimates of the linear dimensions of packed beds necessary to apply the dispersion model.

For miscible displacements in tubes, the minimum time criterion (*1*)

$$\tau_{\min} \geq 0.8 \qquad (36)$$

may also be written in terms of length-to-diameter ratio by taking the real time to be the residence time. Then

$$\frac{L_T}{2a} \geq 0.2\,\frac{(2a)u_m}{D} \qquad (37)$$

is the criterion. If one compares this result to Equation 35, the true criterion is more restrictive than that estimated by Equation 35 and hence, the order of magnitude estimate provided by Bischoff and Levenspiel for packed beds must be used with caution. However, the minimum real time requirement for straight channel systems based on the same equivalent diameter is much smaller than that for tubes and yields a length-to-diameter ratio in much closer agreement with Equation 35.

We have also described in some detail two important effects in porous media—namely, bed capacitance and the instabilities caused by differences in viscosities and densities between displacing and resident phases. From an analysis of the capacitance model, it is clear that systems with large amounts of dead space require significantly larger dimensionless time (or length-to-diameter ratios) for the dispersion model to apply. The effect of viscosity and density differences in unstable situations are such that a dispersion model cannot be used to interpret and extrapolate the results. In capillary tubes, small density differences can have profound effects on the nature of the dispersion and hence, matched density experiments in porous media must be closely examined for the influence of natural convection.

NOMENCLATURE

a = tube radius
b = radius of a tube including stagnant region in Figure 6c
C = mass concentration
D = molecular diffusion coefficient
E = effective axial diffusion coefficient (dispersion coefficient) defined by Equation 3
f_n = nth expansion function in Equation 12
g = acceleration of gravity
h = half width of a parallel plate channel
K = dimensionless dispersion coefficient, $k/(DN_{Pe})$
k = dispersion coefficient
L' = mixing length defined below Equation 5
L = dimensionless mixing length, $DL'/(2a^2u_m)$ for tubes
L_T = length of the system in the main flow direction
N_{Fr} = Froude number
N_{Gr} = Grashof number
N_{Pe} = Peclet number
N_{Re} = Reynolds number
N_{Sc} = Schmidt number
$\bar{n}$ = vector representing the mass flux
n = component of the mass flux vector
P = permeability
p = pressure
q = volumetric flow rate
R = half spacing at the entrance to the diverging channel
R_C = radius of curvature
r = radius radial coordinate
r_A = reaction rate at which A is produced
t = time
U_{ent} = velocity at the entrance to the diverging channel
u = axial velocity component
$\bar{v}$ = vector representing the mass average velocity
v^* = friction velocity defined by Equation 23
x = axial coordinate
x_1 = axial coordinate moving with the mean speed of flow

Greek Letters

α = angle of divergence of the diverging channel
β = $\gamma^2 - 1$
γ = b/a
δ = angular coordinate
$\bullet$ = eddy diffusivity
θ = dimensionless angular coordinate, δ/α
κ = r_i/r_o
λ = friction factor
μ = viscosity
ν = kinematic viscosity, μ/ρ
ρ = density
τ = dimensionless time, tD/a^2 for tubes
τ_s = shear stress
τ_w = shear stress at the wall
ω = mass fraction

Subscript

A = component A
c = critical value
D = mass
d = displacing
$f.p.$ = flat plate
i = inner
M = momentum
m = average
max = maximum
o = outer
r = resident
0 = reference quantity

REFERENCES

(1) Ananthakrishnan, V., Gill, W. N., and Barduhn, A. J., *A.I.Ch.E. J.*, **11**, 1063 (1965).
(2) Aris, R., *Chem. Eng. Sci.*, **10**, 80 (1959).
(3) Aris, R., *ibid.*, **11**, 194 (1959).
(4) Aris, R., *Proc. Roy. Soc.*, **A235**, 67 (1956).
(4A) Aris, R., *ibid.*, **A252**, 538 (1959).
(5) Aris, R., *ibid.*, **A259**, 370 (1960).
(6) Aunicky, Z., *Can. J. Chem. Eng.*, **46**, 27 (1968).
(7) Bailey, H. R., and Gogarty, W. B., *Proc. Roy. Soc.*, **A259**, 352 (1962).
(8) Bailey, H. R., and Gogarty, W. B., *Soc. Petrol. Eng. J.*, **3**, 256 (1963).
(9) Batchelor, G. K., Proc. 2nd Australasian Conference on Hydraulics and Fluid Mechanics, Auckland, Dec. 1965.
(10) Bischoff, K. B., and Levenspiel, O., *Chem. Eng. Sci.*, **17**, 257 (1962).
(11) Blackwell, R. J., *Soc. Petrol. Eng. J.*, **2**, 1 (1962).
(12) Blackwell, R. J., Rayne, J. R., and Terry, W. M., *Trans. AIME*, **216**, 1 (1959).
(13) Bournia, A., Coull, J., and Houghton, G., *Proc. Roy. Soc.*, **A261**, 227 (1961).
(14) Brigham, W. E., Reed, P. W., and Dew, J. N., *Soc. Petrol. Eng. J.*, **1**, 1 (1961).
(15) Carman, P. C., "Flow of Gases through Porous Media," Academic Press, New York, N. Y., 1955.
(16) Carter, D., and Bir, W. G., *Chem. Eng. Progr.*, **58**, 40 (1962).
(17) Cassell, R. E., and Perona, J. J., *A.I.Ch.E. J.*, **15**, 81 (1969).
(18) Coats, K. H., and Smith, B. D., *Soc. Petrol. Eng. J.*, **4**, 73 (1964).
(19) Craig, F. F., Sanderlin, J. L., Moore, D. W., and Geffen, T. M., *Trans. AIME*, **210**, 275 (1957).
(20) Crane, F. E., Kendall, H. A., and Gardner, G. H. F., *Soc. Petrol. Eng. J.*, **3**, 277 (1963).
(20A) Dayan, J., and Levenspiel, O., *Chem. Eng. Sci.*, **23**, 1327 (1968).
(21) Deans, H. A., *Soc. Petrol. Eng. J.*, **3**, 49 (1963).
(22) De Josselin de Jong, A., *Trans. Am. Geophys. Union*, **39**, 67 (1958).
(23) Dougherty, E. L., *Soc. Petrol. Eng. J.*, **3**, 155 (1963).
(24) Dumore, J. M., *ibid.*, **4**, 356 (1964).
(25) Erdogan, M. E., and Chatwin, P. C., *J. Fluid Mech.*, **29**, 465 (1967).
(26) Evans, E. V., and Kenney, C. N., *Proc. Roy. Soc.*, **A284**, 540 (1965).
(27) Flint, L. F., and Eisenklam, P., *Can. J. Chem. Eng.*, **47**, 101 (1969).
(28) Gill, W. N., *Chem. Eng. Sci.*, **22**, 1013 (1967).
(29) Gill, W. N., *Proc. Roy. Soc.*, **A298**, 335 (1967).
(30) Gill, W. N., and Ananthakrishnan, V., *A.I.Ch.E. J.*, **12**, 906 (1966).
(31) Gill, W. N., and Ananthakrishnan, V., *ibid.*, **13**, 801 (1967).
(32) Gill, W. N., Ananthakrishnan, V., and Nunge, R. J., *ibid.*, **14**, 939 (1968).
(33) Gill, W. N., Güceri, Ü., and Nunge, R. J., Office of Saline Water, Research and Development Report No. **443**, June 1969.
(33A) Gill, W. N., "Axial Dispersion with Time Variable Flow in Multiphase Systems," *A.I.Ch.E.J.*, in press, 1969.
(34) Goodknight, R. C., Klikoff, W. A., and Fatt, I., *J. Phys. Chem.*, **64**, 1162 (1960).
(35) Griffiths, A., *Proc. Phys. Soc. London*, **23**, 190 (1911).
(36) Güceri, Ü., "Dispersion in Jeffery-Hamel Flows," M.S. thesis, Clarkson College of Technology, Potsdam, N. Y., June 1968.
(37) Han, C. D., *Chem. Eng. Sci.*, **22**, 837 (1967).
(38) Han, C. D., and Bixler, H. J., *A.I.Ch.E. J.*, **13**, 1058 (1967).
(39) Heller, J. P., *ibid.*, **9**, 452 (1963).
(40) Heller, J. P., *Soc. Petrol. Eng. J.*, **1**, 213 (1961).
(40A) Heller, J. P., *J. Appl. Phys.*, **31**, 1566 (1966).
(40B) Jones, W. M., *Brit. J. Appl. Phys.*, Ser. 2, **1**, 1559 (1968).
(41) Koutsky, J. A., and Adler, R. A., *Can. J. Chem. Eng.*, **42**, 239 (1964).
(42) Koval, E. J., *Soc. Petrol. Eng. J.*, **3**, 145 (1963).
(43) Kramers, H., and Westerterp, K. R., "Elements of Chemical Reactor Design and Operation," Chapman and Hall, London, 1963.
(44) Levenspiel, O., and Bischoff, K. B., "Advances in Chemical Engineering," Vol. 4, pp 98–198, Academic Press, New York, N. Y., 1963.
(45) Levich, V. G., Markin, V. S., and Chismadzhev, Yu. A., *Chem. Eng. Sci.*, **22**, 1351 (1967).
(46) Lin, T.-S., M.S. thesis, Clarkson College of Technology, Potsdam, N. Y., June 1969.
(47) Lu, S.-Z., *ibid.*, in progress.
(47A) Nunge, R. J., Lin, T.-S., and Gill, W. N., "Laminar Dispersion in Curved Tubes and Channels," paper presented at A.I.Ch.E. 62nd Annual Meeting, Washington, D. C., Nov. 1969.
(48) Outmans, H. D., *Soc. Petrol. Eng. J.*, **1**, 298 (1961).
(49) Peaceman, D. W., and Rachford, H. H., *Soc. Petrol. Eng. J.*, **2**, 327 (1962).
(50) Perkins, T. K. and Johnston, O. C., *ibid.*, **3**, 70 (1963).
(51) Perrine, R. L., *ibid.*, **1**, 9 (1961).
(52) Perrine, R. L., *ibid.*, p 17.
(53) Perrine, R. L., *ibid.*, **3**, 205 (1963).
(54) Philip, J. R., *Australian J. Phys.*, **16**, 287 (1963).
(55) Reejhsinghani, N. S., Barduhn, A. J., and Gill, W. N., *A.I.Ch.E. J.*, **14**, 100 (1968).
(56) Reejhsinghani, N. S., Gill, W. N., and Barduhn, A. J., *ibid.*, **12**, 916 (1966).
(57) Saffman, P. A., *Chem. Eng. Sci.*, **11**, 125 (1959).
(58) Saffman, P. A., *J. Fluid Mech.*, **6**, 321 (1959).
(59) Saffman, P. A., *ibid.*, **7**, 194 (1960).
(60) Sankarasubramanian, R., M.S. thesis, Clarkson College of Technology, Potsdam, N. Y., June 1969.
(61) Scheidegger, A. E., "The Physics of Flow Through Porous Media," Macmillan, New York, N. Y., 1960.
(61A) Schowalter, W. R., *A.I.Ch.E.J.*, **11**, 99 (1965).
(62) Shulman, H. L., and Mellish, W. G., *A.I.Ch.E. J.*, **13**, 1137 (1967).
(62A) Sittel, C. N., Threadgill, W. D., and Schnelle, K. B., IND. ENG. CHEM. FUNDAMENTALS, **7**, 39 (1968).
(63) Slobod, R. L., and Howelett, W. E., *Soc. Petrol. Eng. J.*, **4**, 1 (1964).
(64) Slobod, R. L., and Thomas, R. A., *ibid.*, **3**, 9 (1963).
(65) Smith, J. V., M.S. thesis, Univ. of Tennessee, Knoxville, Tenn., June 1967.
(66) Taylor, G. I., *Proc. Phys. Soc. London*, **67**, 857 (1954).
(67) Taylor, G. I., *Proc. Roy. Soc.*, **A219**, 186 (1953).
(68) Taylor, G. I., *ibid.*, **A223**, 446 (1954).
(69) Taylor, G. I., *ibid.*, **A225**, 473 (1954).
(70) Taylor, H. M., and Leonard, E. F., *A.I.Ch.E. J.*, **11**, 686 (1965).
(71) Taylor, H. M., Ph.D. thesis, Columbia University, New York, N. Y., 1967.
(72) Tichacek, L. J., Barkelew, C. H., and Baron, T., *A.I.Ch.E. J.*, **3**, 439 (1957).
(73) Turner, G. A., *Chem. Eng. Sci.*, **7**, 156 (1958).
(74) Turner, G. A., *ibid.*, **10**, 14 (1959).
(75) Turner, J. C. R., *British Chem. Eng.*, **9**, 377 (1964).
(76) Van Deemter, J. J., Broeder, J. J., and Lauwerier, H. A., *Appl. Sci. Res.*, **5A**, 374 (1956).
(77) Van der Poel, C., *Soc. Petrol. Eng. J.*, **2**, 317 (1962).
(78) Von Rosenberg, D. U., *A.I.Ch.E. J.*, **2**, 55 (1956).
(79) Wooding, R. A., *Proc. Roy. Soc.*, **A252**, 120 (1959).
(80) Wooding, R. A., *ZAMP*, **13**, 256 (1962).
(81) Wright, D. E., *J. Hydral. Div., Proc. ASCE*, **94**, 851 (1968).